IEEE Transactions on Antennas and Propagation

Upper Bounds and Design Guidelines for Realizing Uncorrelated Ports on Multi-Mode Antennas Based on Symmetry Analysis of Characteristic Modes

Authors:
Nikolai Peitzmeier
Dirk Manteuffel

Suggested Citation:
N. Peitzmeier and D. Manteuffel, "Upper Bounds and Design Guidelines for Realizing Uncorrelated Ports on Multi-Mode Antennas Based on Symmetry Analysis of Characteristic Modes", *IEEE Transactions on Antennas and Propagation*, vol. 67, no. 6, pp. 3902-3914, June 2019.

Upper Bounds and Design Guidelines for Realizing Uncorrelated Ports on Multi-Mode Antennas Based on Symmetry Analysis of Characteristic Modes

Nikolai Peitzmeier, *Student Member, IEEE,* and Dirk Manteuffel, *Member, IEEE*

***Abstract*—The design of multi-port antennas for MIMO applications utilizing characteristic modes is investigated. For good MIMO performance, uncorrelated antenna ports are generally required. In order to analyze the port correlation, symmetry analysis based on group theory and matrix representations is applied to the theory of characteristic modes. The characteristic surface current densities act as basis functions of the irreducible representations of the symmetry group of the antenna. Current densities belonging to different representations or belonging to different rows of the same representation are orthogonal to each other and can thus be excited separately. Therefore, an upper bound for the number of uncorrelated antenna ports can be derived for a given antenna structure based on the symmetry analysis of the characteristic modes. Furthermore, design guidelines on which antenna geometry to choose in order to realize a given number of uncorrelated antenna ports and on how to implement these ports can be deduced. The concept is illustrated by means of examples.**

***Index Terms*—Antenna theory, group theory, characteristic modes, multiple-input multiple-output (MIMO), multi-mode antenna, symmetry.**

I. Introduction

THE concept of multi-mode antennas based on the theory of characteristic modes [1]–[3] has proved to be a promising approach in order to enable multiple-input multiple-output (MIMO) techniques in spatially restricted environments. With this concept, a multi-port antenna can be created on a single antenna structure, thereby optimally utilizing the given space. The numerous examples reported in literature include the design of multi-port mobile terminal antennas [4]–[7] as well as base station antennas [8], [9].

The reason that characteristic modes are most suitable for MIMO applications is rooted in their orthogonality properties. These state that the characteristic far fields are orthogonal to each other [2], offering pattern and polarization diversity. Therefore, the design of multi-mode antennas aims at exciting different sets of characteristic modes with different antenna ports. This way, uncorrelated ports are realized on a single antenna structure.

Regarding the excitation of characteristic modes, the following nomenclature is employed: A set of characteristic modes is said to be excited if the total excited current density is a weighted sum of the corresponding modal current densities alone. A single mode is said to be excited if its modal current density is part of this weighted sum.

In recent publications, MIMO antenna designs with up to four ports realized by means of characteristic mode analysis can be found [4]–[10]. The antenna ports are typically defined by inspecting the characteristic surface current densities and/or the characteristic near fields [11]. For example, in [9] a multi-mode antenna with four ports was designed based on the characteristic mode analysis of a square plate. Excitation slots are placed where maxima of the characteristic surface current densities occur.

The question arises whether even more antenna ports can be implemented if more characteristic modes are taken into account. As proposed in [12], [13], this can prove useful for future techniques such as massive MIMO. In [14], the authors showed that a typical smart phone chassis can offer a large number of modes, depending on the operating frequency. However, it was also shown that the number of uncorrelated antenna ports, which can be realized based on characteristic mode analysis, is apparently limited and that this limitation is related to the symmetry of the underlying antenna structure. Furthermore, it was found that the port definition by simply inspecting the characteristic surface current densities becomes rather cumbersome if a large number of characteristic modes is significant. Nevertheless, the optimized port definition in [14] seems to be related to the symmetry of the antenna as well. These observations raise the fundamental questions how the symmetry of an antenna affects its characteristic modes and whether there is an upper bound for the number of uncorrelated antenna ports. At this point, it is noteworthy that the designs presented in [4]–[10] all originate from symmetric structures. In particular, the importance and the advantages of symmetry for designing multi-mode antennas are explicitly recognized in [4], [8], [10] as well as in [15], [16].

Due to the questions raised above, it is purposeful to get a fundamental understanding of how the characteristic modes are affected by the symmetry of an antenna in order to enable a systematic design of multi-mode antennas with a high number of uncorrelated antenna ports. Symmetry analysis was introduced to the theory of characteristic modes in [17]. The aim was to improve the characteristic mode computation of symmetric structures by simplifying the impedance matrix based on symmetry considerations. As the underlying mathematical tools, group theory and matrix representations were applied to the theory of characteristic modes. More recently,

This work was supported by Deutsche Forschungsgemeinschaft (DFG) within the priority program SPP 1655 under grant MA 4981/4-2.

The authors are with the Institute of Microwave and Wireless Systems, Leibniz University Hannover, Hannover 30167, Germany, (e-mail: peitzmeier@hft.uni-hannover.de; manteuffel@hft.uni-hannover.de).

these mathematical methods were used in order to understand crossing avoidances occurring during eigenvalue tracking of characteristic modes [18], [19].

Inspired by these works, this paper aims at gaining fundamental insight into the influence of a structure's symmetry on its characteristic modes. In particular, the consequences of symmetry on the selective excitation of characteristic modes are investigated. It will be shown that, by applying symmetry analysis, the number of feasible uncorrelated antenna ports can be predicted. Furthermore, instructions on what antenna geometry to choose and how to implement the feed network can be derived.

To this end, first the mathematical description of symmetry by means of group theory and matrix representations is introduced in section II. These tools are then applied to the theory of characteristic modes in section III. Based on the presented theory, in section IV the selective excitation of characteristic modes for MIMO applications is discussed. The theoretical findings are illustrated by numerical examples in section V. The paper concludes with a summary and a discussion in section VI.

II. Mathematical Description of Symmetry

Intuitively, a symmetry operation is a transformation that maps a geometric object onto itself, i.e. it leaves the object invariant. Symmetry operations can mathematically be described as coordinate transformations, e.g. rotations or reflections. The symmetry operations that leave a specific object invariant form a mathematical group, the symmetry group of the object [20].

A. Group Theory

Most symmetric objects encountered in antenna engineering have a finite number of symmetry operations. The corresponding symmetry group is said to be finite and the number of group elements is called its order. One group element is always the unit element, representing the identical transformation. The other elements are the symmetry operations. There is a group multiplication which for symmetry groups describes the execution of symmetry operations in succession. The multiplication is associative, but not generally commutative. Every multiplication of group elements yields again an element of the group. For each element there is an inverse element so that the multiplication yields the unit element [21].

As an example, the infinitely thin square plate in Fig. 1 is considered. Its symmetry group is D_4 (Schoenfliess notation [22]). In addition to the unit element E, it consists of three rotations about the z-axis (principal rotation axis): By 90 ° (C_{4z}), by −90 ° (C_{4z}^{-1}), and by 180 ° (C_{2z}). Additionally, there are four rotations by 180 ° about axes perpendicular to the z-axis: The x-axis (C_{2x}), the y-axis (C_{2y}), the diagonal a (C_{2a}), and the diagonal b (C_{2b}) [22]. The eight group elements are listed in Table I.

Symmetry groups that leave one point of the coordinate system invariant (usually the origin) are called point groups. The symmetry of various antenna types can be described with point groups, e.g. dipole and patch antennas. The symmetry operations that can be elements of a point group are proper rotations and improper rotations (inversion, reflections, and rotoreflections) [22]. In three-dimensional Euclidean space, these operations can be expressed by orthogonal transformation matrices $\mathbf{R}(T)$ that transform the original coordinates $\mathbf{r} = (x, y, z)^T$ into the transformed coordinates $\mathbf{r}' = (x', y', z')^T$ [20]:

$$\mathbf{r}' = \mathbf{R}(T)\,\mathbf{r}, \tag{1}$$

where T is an element of the symmetry group. The symmetry group D_4 of the square consists of only proper rotations. The corresponding rotation matrices are listed in Table I. For example, the rotation by 180 ° about the z-axis (C_{2z}) leaves the z-axis invariant, but inverts the x- and y-axis. In the new coordinates, the object looks exactly the same as in the original coordinates. It should be noted that the rotation matrices form

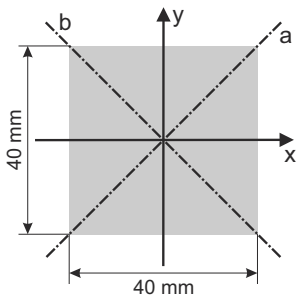

Fig. 1. Square plate and coordinate system.

TABLE I
Group Elements, Rotation Matrices, and Transformation Operators of the Symmetry Group D_4 of a Square Plate

T	$\mathbf{R}(T)$	$P(T)\,\mathbf{f}(\mathbf{r})$
E	$\begin{pmatrix}1&0&0\\0&1&0\\0&0&1\end{pmatrix}$	$\begin{pmatrix}f_x(x,y,z)\\f_y(x,y,z)\\f_z(x,y,z)\end{pmatrix}$
C_{4z}	$\begin{pmatrix}0&1&0\\-1&0&0\\0&0&1\end{pmatrix}$	$\begin{pmatrix}f_y(-y,x,z)\\-f_x(-y,x,z)\\f_z(-y,x,z)\end{pmatrix}$
C_{4z}^{-1}	$\begin{pmatrix}0&-1&0\\1&0&0\\0&0&1\end{pmatrix}$	$\begin{pmatrix}-f_y(y,-x,z)\\f_x(y,-x,z)\\f_z(y,-x,z)\end{pmatrix}$
C_{2z}	$\begin{pmatrix}-1&0&0\\0&-1&0\\0&0&1\end{pmatrix}$	$\begin{pmatrix}-f_x(-x,-y,z)\\-f_y(-x,-y,z)\\f_z(-x,-y,z)\end{pmatrix}$
C_{2x}	$\begin{pmatrix}1&0&0\\0&-1&0\\0&0&-1\end{pmatrix}$	$\begin{pmatrix}f_x(x,-y,-z)\\-f_y(x,-y,-z)\\-f_z(x,-y,-z)\end{pmatrix}$
C_{2y}	$\begin{pmatrix}-1&0&0\\0&1&0\\0&0&-1\end{pmatrix}$	$\begin{pmatrix}-f_x(-x,y,-z)\\f_y(-x,y,-z)\\-f_z(-x,y,-z)\end{pmatrix}$
C_{2a}	$\begin{pmatrix}0&1&0\\1&0&0\\0&0&-1\end{pmatrix}$	$\begin{pmatrix}f_y(y,x,-z)\\f_x(y,x,-z)\\-f_z(y,x,-z)\end{pmatrix}$
C_{2b}	$\begin{pmatrix}0&-1&0\\-1&0&0\\0&0&-1\end{pmatrix}$	$\begin{pmatrix}-f_y(-y,-x,-z)\\-f_x(-y,-x,-z)\\-f_z(-y,-x,-z)\end{pmatrix}$

a group themselves, which is isomorphic to the symmetry group.

B. Transformation Operators

Up to this point, the transformation of the coordinate system due to symmetry operations has been described. When working with characteristic modes, current densities on the surface of an antenna structure are typically of particular interest. It is therefore important to know how a vector-valued function $\mathbf{f}(\mathbf{r}) = (f_x(\mathbf{r}), f_y(\mathbf{r}), f_z(\mathbf{r}))^T$ defined in a given coordinate system is affected by a transformation of the coordinate system due to a symmetry operation. This is accomplished by transformation operators [20]. The transformed function $\mathbf{f}'$ can be expressed in terms of the original coordinates using the transformation matrix $\mathbf{R}(T)$:

$$\mathbf{f}'(\mathbf{r}) = P(T)\,\mathbf{f}(\mathbf{r}) = \mathbf{R}\mathbf{f}\left(\mathbf{R}^{-1}(T)\,\mathbf{r}\right). \tag{2}$$

$P(T)$ is called the transformation operator of element T operating on $\mathbf{f}$. It should be emphasized that these operators directly operate on functions instead of coordinates [23]. The transformation operators of the square are included in Table I. They explicitly describe the rotation of an arbitrary function due to the symmetry operations in the given coordinate system. As an example, for the rotation by 180 ° about the z-axis (C_{2z}) the x- and y-components of the vector-valued function $\mathbf{f}$ are inverted, whereas the z-component remains invariant. Likewise, the x- and y-dependencies are inverted, whereas the z-dependency remains invariant.

C. Basis Functions and Matrix Representations

For every symmetry group there exist special sets of linearly independent (vector-valued) functions $\boldsymbol{\psi}$ that transform into linear combinations of each other when operated on by the transformation operators [23]:

$$P(T)\,\boldsymbol{\psi}_n^{(p)}(\mathbf{r}) = \sum_{m=1}^{d_p} \Gamma_{mn}^{(p)}(T)\,\boldsymbol{\psi}_m^{(p)}(\mathbf{r}), \quad n = 1, 2, \ldots, d_p. \tag{3}$$

The function $\boldsymbol{\psi}_n^{(p)}$ is called the n-th basis function of the p-th d_p-dimensional representation of the symmetry group. The effect of the symmetry operation T on $\boldsymbol{\psi}_n^{(p)}$ is equal to a linear combination of the d_p basis functions $\boldsymbol{\psi}_1^{(p)}$ to $\boldsymbol{\psi}_{d_p}^{(p)}$. The weighting coefficients $\Gamma_{mn}^{(p)}(T)$ are elements of a d_p-dimensional square matrix $\boldsymbol{\Gamma}^{(p)}(T)$. (It has to be highlighted here that n is the row index [20].) Equation (3) describes the effect of a transformation operator on a basis function and the basis function is said to transform according to the n-th row of the p-th representation.

The matrix $\boldsymbol{\Gamma}^{(p)}(T)$ is called the representation matrix of the p-th representation for the symmetry operation T. A d_p-dimensional representation is a group homomorphic to the symmetry group that assigns a square matrix of dimension d_p to each element of the symmetry group [23]. For a given group, there is generally an infinite number of matrix representations. However, for a finite group there is a finite number of so-called irreducible representations of minimal dimension from which all other representations can be derived [20]. The irreducible representations of a finite group are unique up to a similarity transformation. For these reasons, it is purposeful to work only with the irreducible representations.

The representation matrices can usually not be found in the literature. Instead, character tables are given (e.g. [22]). The character $\chi^{(p)}(T)$ of a representation is the trace of the representation matrix [20]:

$$\chi^{(p)}(T) = \operatorname{tr}\left(\boldsymbol{\Gamma}^{(p)}(T)\right). \tag{4}$$

For one-dimensional representations, the characters are the representation matrices.

The symmetry group of the square plate has five irreducible representations. The representation matrices are given in Table II [20]. They describe how the basis functions transform under the symmetry operations. The first four representations are one-dimensional and their matrices are thus equal to the characters. The fifth representation, however, is two-dimensional and consists therefore of two-dimensional matrices. This has the consequence that a pair of basis functions belongs to this representation. An example for a basis function transforming according to the first row of the fifth representation is $\boldsymbol{\psi}_1^{(5)}(x, y, z) = (|x|, 0, 0)^T$. Its partner function is $\boldsymbol{\psi}_2^{(5)}(x, y, z) = (0, |y|, 0)^T$, which can be checked by manual inspection.

The basis functions of the irreducible representations have very important orthogonality properties [20]:

$$\left\langle \boldsymbol{\psi}_m^{(p)}(\mathbf{r}), \boldsymbol{\psi}_n^{(q)}(\mathbf{r}) \right\rangle = 0, \tag{5}$$

unless $p = q$ and $m = n$, where $\langle\cdot\rangle$ denotes an inner product of L^2. This equation means that basis functions belonging to different irreducible representations and basis functions belonging to different rows of the same irreducible representation are orthogonal to each other. This orthogonality theorem is of great importance for the selective excitation of characteristic modes, as will be shown in the next sections.

III. Symmetry of Characteristic Modes

In this section, the connection of the symmetry analysis to the theory of characteristic modes is established. The theory of characteristic modes for perfectly electrically conducting (PEC) structures is based on the following eigenvalue problem [2]:

$$X(\mathbf{J}_n(\mathbf{r})) = \lambda_n R(\mathbf{J}_n(\mathbf{r})), \tag{6}$$

where λ_n denotes the n-th eigenvalue and $\mathbf{J}_n$ the n-th characteristic surface current density (eigenfunction). The operators R and X are the real and imaginary part, respectively, of the impedance operator Z derived from the electric field integral equation (EFIE) and the electric field boundary condition for perfect electric conductors.

In [17], it is demonstrated that the impedance operator is invariant under the symmetry operations of the underlying PEC structure. Applying a transformation operator of the symmetry group to the impedance operator yields

$$P(T)\,Z(\mathbf{J}_n(\mathbf{r})) = Z(P(T)\,\mathbf{J}_n(\mathbf{r})) = Z(\mathbf{J}_n'(\mathbf{r})). \tag{7}$$

TABLE II
MATRIX REPRESENTATIONS OF SYMMETRY GROUP D_4

D_4	E	C_{4z}	C_{4z}^{-1}	C_{2z}	C_{2x}	C_{2y}	C_{2a}	C_{2b}
$\Gamma^{(1)}$	1	1	1	1	1	1	1	1
$\Gamma^{(2)}$	1	1	1	1	-1	-1	-1	-1
$\Gamma^{(3)}$	1	-1	-1	1	1	1	-1	-1
$\Gamma^{(4)}$	1	-1	-1	1	-1	-1	1	1
$\Gamma^{(5)}$	$\begin{pmatrix}1 & 0\\0 & 1\end{pmatrix}$	$\begin{pmatrix}0 & -1\\1 & 0\end{pmatrix}$	$\begin{pmatrix}0 & 1\\-1 & 0\end{pmatrix}$	$\begin{pmatrix}-1 & 0\\0 & -1\end{pmatrix}$	$\begin{pmatrix}1 & 0\\0 & -1\end{pmatrix}$	$\begin{pmatrix}-1 & 0\\0 & 1\end{pmatrix}$	$\begin{pmatrix}0 & 1\\1 & 0\end{pmatrix}$	$\begin{pmatrix}0 & -1\\-1 & 0\end{pmatrix}$

The transformation operator is said to commute with the impedance operator [23]. This result is now applied to (6), yielding [17]

$$X\left(P\left(T\right)\mathbf{J}_n\left(\mathbf{r}\right)\right) = \lambda_n R\left(P\left(T\right)\mathbf{J}_n\left(\mathbf{r}\right)\right). \tag{8}$$

This means that all transformed surface current densities (including the identity transformation) are eigenfunctions with the same eigenvalue.

Any eigenfunction of a d-fold degenerate eigenvalue can be expressed as a linear combination of d linearly independent eigenfunctions belonging to that eigenvalue [24]. Thus, a transformed eigenfunction can be written as

$$P\left(T\right)\mathbf{J}_n\left(\mathbf{r}\right) = \sum_{m=1}^{d} a_{mn}\mathbf{J}_m\left(\mathbf{r}\right), \quad n = 1, 2, \ldots, d \tag{9}$$

with the weighting coefficients a_{mn}. For example, if λ_n is twofold degenerate, then every transformed characteristic surface current density can be expressed as a linear combination of the two characteristic surface current densities belonging to this eigenvalue solved from (6), which are linearly independent by definition [24]. In this case, the coefficients a_{mn} can be collected into a two-dimensional square matrix.

As a matter of fact, this defines a representation (cf. (3)). The eigenfunctions (characteristic surface current densities) form basis functions of the irreducible representations of the symmetry group. A detailed proof can be found in [20] or [25]. This connection between the theory of characteristic modes and the theory of symmetry will be made use of in the following section.

IV. SELECTIVE EXCITATION OF CHARACTERISTIC MODES

In the previous section, it was shown that the characteristic surface current densities act as basis functions of the irreducible representations of the symmetry group which leaves the impedance operator invariant. The orthogonality properties of basis functions (5) will now be applied to the excitation of characteristic modes.

An arbitrary surface current density $\mathbf{J}(\mathbf{r})$ on a PEC-structure can be decomposed into a weighted sum of its characteristic surface current densities [2]:

$$\mathbf{J}\left(\mathbf{r}\right) = \sum_n \alpha_n \mathbf{J}_n\left(\mathbf{r}\right) = \frac{\left\langle \mathbf{J}_n\left(\mathbf{r}\right), \mathbf{E}_{\text{inc}}\left(\mathbf{r}\right)\right\rangle}{1 + j\lambda_n}\mathbf{J}_n\left(\mathbf{r}\right), \tag{10}$$

where α_n is called the modal weighting coefficient. Its numerator is called the modal excitation coefficient, which takes into account the excitation by an incident electric field $\mathbf{E}_{\text{inc}}$, which may for instance be impressed locally by a concentrated antenna port. The inner product is now explicitly defined as

$$\left\langle \mathbf{J}_n\left(\mathbf{r}\right), \mathbf{E}_{\text{inc}}\left(\mathbf{r}\right)\right\rangle = \oiint_{S'} \mathbf{J}_n\left(\mathbf{r}\right)\cdot\mathbf{E}_{\text{inc}}\left(\mathbf{r}\right)\mathrm{d}S', \tag{11}$$

where the integration is taken over the surface S' of the underlying PEC structure.

From (10) it is deduced that a necessary criterion for a characteristic mode to be efficiently excited is that its eigenvalue must be close to zero. Additionally, the modal excitation coefficient needs to be maximized. This is accomplished if the incident electric field is collinear to the characteristic surface current density. By contrast, if the two functions were orthogonal to each other, the characteristic mode would not be excited at all.

In the design of multi-mode antennas for MIMO applications, it would be the ideal case to design an excitation that efficiently excites exactly one mode and is orthogonal to all other modes. However, in [14] it was shown that this may generally not be possible as certain characteristic surface current densities may be correlated. The characteristic current correlation coefficient ρ_{mn} measures the correlation between the m-th and the n-th characteristic surface current density:

$$\rho_{mn} = \frac{\left\langle \mathbf{J}_m\left(\mathbf{r}\right), \mathbf{J}_n\left(\mathbf{r}\right)\right\rangle}{\left\|\mathbf{J}_m\left(\mathbf{r}\right)\right\|\left\|\mathbf{J}_n\left(\mathbf{r}\right)\right\|}, \tag{12}$$

where $\|\cdot\|$ denotes the norm induced by the definition of the inner product in (11). The correlation is a measure for the similarity of surface current densities, especially regarding the positions of local maxima and nulls, which are typical locations for placing excitation elements [11]. This has the consequence that, if the surface current densities of two modes are correlated, an antenna port that is intended to excite the first mode will potentially also excite the second one. A second antenna port that is intended to excite the second mode will in principle also excite the first mode so that both antenna ports will potentially excite the same modes. Therefore, both ports will be correlated which is to be avoided for MIMO applications [26].

The port correlation is measured by means of the envelope correlation coefficients (ECC) [27]:

$$\text{ECC}_{uv} = \frac{\frac{1}{2Z_0}\oiint_S \mathbf{E}_u\cdot\mathbf{E}_v^*\mathrm{d}S}{\sqrt{P_{\text{rad},u}}\sqrt{P_{\text{rad},v}}}, \tag{13}$$

where the integration is taken over a closed surface S in the far field encompassing the antenna. $\mathbf{E}_u$ and $\mathbf{E}_v$ denote the total radiated electric far fields excited by the u-th and v-th antenna

port, respectively, Z_0 denotes the wave impedance of free space, $P_{\text{rad},u;v}$ the radiated power of the u-th and v-th port, respectively, and * the complex conjugate. The radiated far fields can be expressed by the characteristic far fields and the modal weighting coefficients [2]:

$$\text{ECC}_{uv} = \frac{\frac{1}{2Z_0} \oiint_S \sum_m \alpha_{m,u} \mathbf{E}_m \cdot \sum_n \alpha^*_{n,v} \mathbf{E}^*_n \mathrm{d}S}{\sqrt{P_{\text{rad},u}} \sqrt{P_{\text{rad},v}}}. \quad (14)$$

Due to the orthogonality of the characteristic far fields [2], this reduces to

$$\text{ECC}_{uv} = \frac{\sum_n \alpha_{n,u} \alpha^*_{n,v} \frac{1}{2Z_0} \oiint_S \|\mathbf{E}_n\|^2 \mathrm{d}S}{\sqrt{P_{\text{rad},u}} \sqrt{P_{\text{rad},v}}}. \quad (15)$$

If the characteristic modes are normalized to radiate unit power [2], this can be simplified further to

$$\text{ECC}_{uv} = \frac{\sum_n \alpha_{n,u} \alpha^*_{n,v}}{\sqrt{P_{\text{rad},u}} \sqrt{P_{\text{rad},v}}} = \sum_n b_{n,u} b^*_{n,v}, \quad (16)$$

where $b_{n,u;v}$ are the normalized modal weighting coefficients of the u-th and v-th antenna port, respectively, as defined in [27]:

$$b_n = \frac{\alpha_n}{\sqrt{P_{\text{rad}}}}, \quad (17)$$

which can also be interpreted as the correlation coefficients between the total radiated far field excited by a port and the modal far fields.

Equation (16) demonstrates the fact that antenna ports are uncorrelated if they excite mutually exclusive sets of characteristic modes, i.e. $b_{n,u} = 0$ if $b_{n,v} \neq 0$ and vice versa. The current correlation introduced in (12) is a qualitative indicator whether two characteristic modes can be excited separately.

As the characteristic surface current densities are basis functions of the irreducible representations of the symmetry group of the antenna structure, the current correlation defined in (12) is dictated by the orthogonality theorem in (5). Therefore, characteristic surface current densities of different representations and characteristic surface current densities of different rows of the same representation are orthogonal to each other. They may thus be excited separately and the number of feasible uncorrelated antenna ports is apparently governed by the number and dimensions of the irreducible representations, i.e. there is an upper bound for realizing uncorrelated antenna ports on multi-mode antennas.

Furthermore, the modal excitation coefficient in (10) indicates that, in order to excite the characteristic modes of a specific irreducible representation, the incident electric field, too, should be a basis function of that representation (symmetric excitation). In this case, the modal excitation coefficient has the form of (5) so that the excitation cannot excite modes belonging to other representations or other rows of the same representation. Conversely, if the incident electric field is applied asymmetrically, a mixture of characteristic modes belonging to different representations will be excited, reducing the number of uncorrelated antenna ports that can be realized. Based on these observations, instructions for creating the maximum number of uncorrelated antenna ports can be derived from the symmetry analysis.

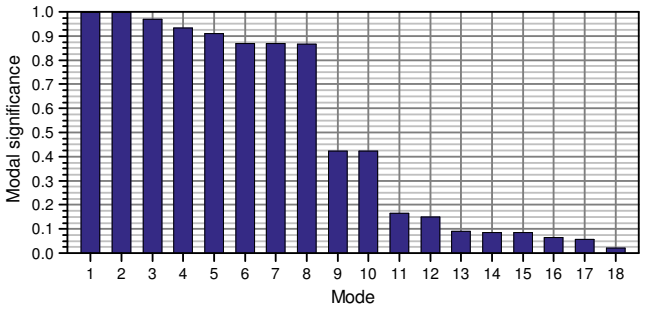

Fig. 2. Modal significances of square PEC plate at 7.25 GHz.

V. Numerical Examples

In this section, numerical examples will be discussed in order to illustrate the fundamental properties and relationships introduced in the previous section and demonstrate the usefulness of the presented theory for the design of multi-mode antennas.

The characteristic modes are computed [3] using an in-house method of moments software which is implemented in MATLAB. It is based on a modified version of the code presented in [28] for the method of moments, built-in MATLAB functions for solving the generalized eigenvalue problem as well as advanced tracking algorithms [29]. In particular, for all simulation models a symmetric mesh is used that is invariant under the symmetry operations of the respective structure (cf. [19]). All modal analyses are conducted at 7.25 GHz. (It is emphasized that the symmetry analysis is frequency-independent.)

A. Square Plate

In order to illustrate the basic procedure of the symmetry analysis and its application to the excitation of characteristic modes, an infinitely thin square PEC plate of dimensions 40 mm×40 mm is analyzed (see Fig. 1). Its symmetry group is D_4, which has already been introduced in section II.

The corresponding irreducible representations are given in Table II. There are four one-dimensional and one two-dimensional representations. According to the previous sections, the characteristic surface current densities that act as basis functions of different representations and those which form a pair of basis functions of the two-dimensional representation are orthogonal to each other. This results in a total of six mutually orthogonal sets of characteristic modes and thus six uncorrelated antenna ports are expected to be feasible.

The two-dimensional representation yields another important property of the characteristic modes: Two modes that form a pair of basis functions for this representation are degenerate, i.e. they have the same eigenvalue independent of frequency [17].

To verify these statements, a modal analysis of the square plate is now conducted. For this purpose, the square plate is discretized into a symmetric mesh consisting of 2472 triangles. This relatively fine mesh is chosen in order to get detailed current plots. It should be noted that the results derived in the following paragraphs are basically independent of the mesh

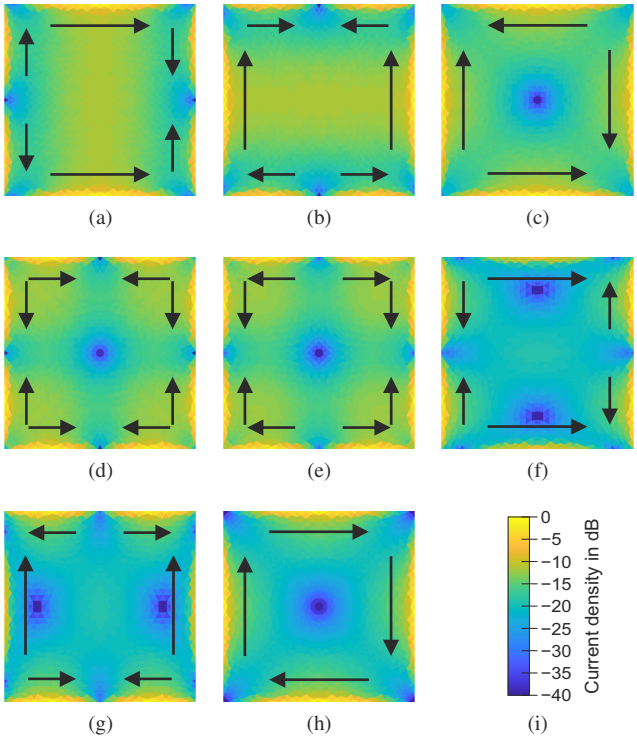

Fig. 3. Normalized surface current densities of significant characteristic modes of square PEC plate at 7.25 GHz with principal current directions denoted by arrows. (a)-(h) Modes 1 to 8. (i) Colorbar.

TABLE III
ASSIGNMENT OF CHARACTERISTIC MODES OF SQUARE PEC PLATE TO IRREDUCIBLE REPRESENTATIONS OF SYMMETRY GROUP D_4

Representation	Characteristic modes
$\Gamma^{(1)}$	4; 12
$\Gamma^{(2)}$	8; 13; 17
$\Gamma^{(3)}$	5; 11
$\Gamma^{(4)}$	3; 16; 18
$\Gamma^{(5)}$	1-2; 6-7; 9-10; 14-15

density as long as the symmetry of the antenna is represented accordingly and the characteristic modes are calculated accurately.

In the first step, the modal significances [30] as shown in Fig. 2 are examined. 18 characteristic modes have been taken into account. Modes with modal significances greater than $1/\sqrt{2}$ (eigenvalues between -1 and 1) are considered significant, i.e. their eigenvalues are close enough to zero so that they are suitable for excitation. Modes 1 to 8 fulfill this requirement. Furthermore, the mode pairs 1-2, 6-7, 9-10, and 14-15, respectively, can be recognized as degenerate mode pairs as they have the same modal significances (eigenvalues). Due to this, these mode pairs can already be identified as basis functions of the two-dimensional fifth representation.

In order to assign all characteristic modes to the irreducible representations, their surface current densities are inspected. The current densities of the significant modes are displayed in Fig. 3, where the principal current directions are denoted by the arrows. Modes 3 (Fig. 3(c)), 4 (Fig. 3(d)), 5 (Fig. 3(e)), and 8 (Fig. 3(h)) act as basis functions of the different one-

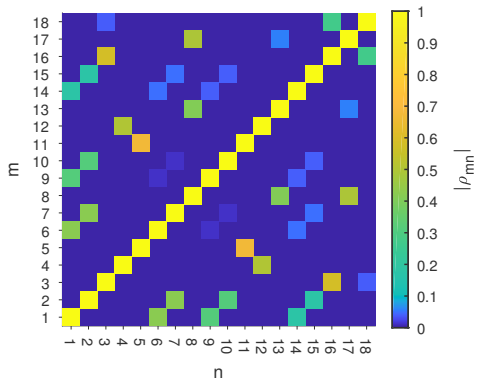

Fig. 4. Characteristic current correlation of square PEC plate at 7.25 GHz.

dimensional representations of the square plate. This can be checked by applying all operations of the symmetry group to the current densities. For example, mode 4 (Fig. 3(d)) is invariant under all symmetry operations (multiplication with 1) and thus belongs to the first representation. In contrast, mode 8 (Fig. 3(h)) is invariant under all rotations about the z-axis, but is inverted for all other rotations (multiplication with -1) and is therefore a basis function of the second representation.

The pairs of degenerate modes 1-2 (Fig. 3(a) and (b)) and 6-7 (Fig. 3(f) and (g)) act as basis functions for the two-dimensional representation, as expected. Their transformations are described by two-dimensional representation matrices (Table II). Modes 1 and 6 transform according to the first row of the representation and modes 2 and 7 transform according to the second row (see (3)). For instance, a rotation by 180 ° about the x-axis (C_{2x}) leaves mode 1 invariant, but inverts mode 2. In particular, the basis functions transform into each other for some operations. This is e.g. the case for the rotation (of the coordinate system) by 90 ° about the z-axis (C_{4z}), where mode 1 becomes the inverted mode 2 and mode 2 becomes mode 1. (This is equal to a rotation of the current densities themselves by −90 °.) The assignment of all 18 characteristic modes to the representations based on the inspection of the surface current densities is summarized in Table III.

In the next step, the characteristic current correlation as defined in (12) is evaluated, which is shown in Fig. 4. It is clearly visible that current densities belonging to different irreducible representations are orthogonal to each other. In particular, the current densities belonging to different rows of the two-dimensional representation are mutually orthogonal. Thus, it is confirmed that the characteristic surface current densities act as basis functions of the irreducible representations and that they fulfill the orthogonality theorem in (5). Furthermore, it can be observed that current densities belonging to the same representation are correlated. The actual value of the correlation coefficient is not defined by the orthogonality theorem and there may be some cases where it is comparatively small.

Now that the characteristic modes have been sorted according to their symmetry properties, excitations for the modes can be designed based on the symmetry analysis. As stated in section IV, the excitation has to be designed in such a way

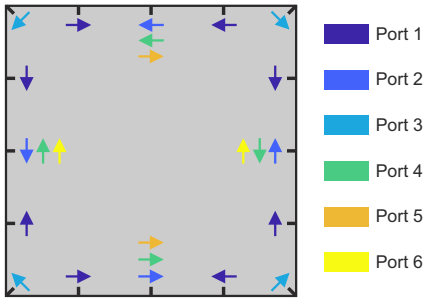

Fig. 5. Port configuration on square PEC plate.

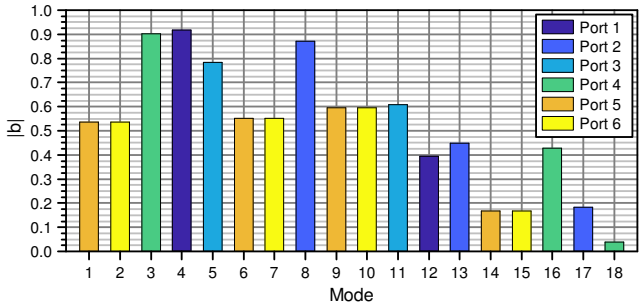

Fig. 6. Absolute values of normalized modal weighting coefficients of square PEC plate excited according to Fig. 5 at 7.25 GHz.

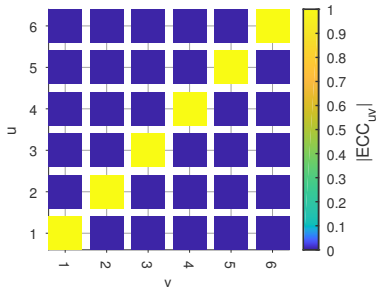

Fig. 7. Envelope correlation coefficients (ECC) of square PEC plate excited according to Fig. 5 at 7.25 GHz.

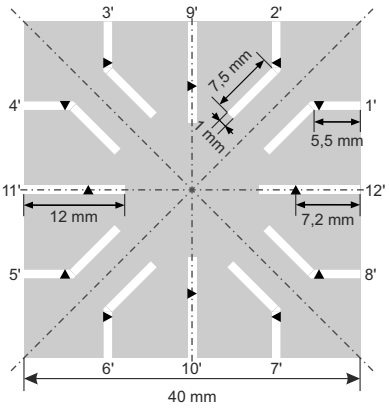

Fig. 8. Port configuration of square PEC plate with excitation slots. The feed points within the slots (black arrows) are labelled by primed numbers.

that the corresponding incident electric field is a basis function of the representation the mode which is intended to be excited belongs to. For example, an excitation that is intended to excite mode 4, which belongs to the first representation, has to be invariant under all symmetry operations of the group.

For the analysis of the excitation, voltage sources, implemented as gap sources in the method of moments [28], are employed. One antenna port consists of several voltage sources which are placed on the plate and driven in such a way that they fulfill the symmetry requirements of the respective representation. One possible port configuration is shown in Fig. 5. The voltage gap sources are marked by the small black strips and the directions of the applied voltages (relative phase) are denoted by arrows. All sources have the same amplitude. Those sources which belong to the same antenna port have the same color. In this configuration, some sources are used by more than one port. As an example, antenna port 1 is intended to excite mode 4. It consists of eight voltage sources which are positioned and driven in such a way that it is invariant under all symmetry operations of the square plate.

In order to evaluate which characteristic modes are excited by the previously defined antenna ports, the normalized modal weighting coefficients introduced in (17) are used. The normalized modal weighting coefficients (absolute value) of the square PEC plate excited according to Fig. 5 are depicted in Fig. 6. Every port excites a different set of characteristic modes. Each set only consists of modes belonging to the same representation or the same row of the two-dimensional representation, respectively (see Table III). This is due to the fact that both the incident electric fields impressed by the ports and the characteristic surface current densities are basis functions of the irreducible representations of the symmetry group of the square plate and thus the orthogonality theorem holds. As a consequence, the antenna ports are uncorrelated which is confirmed by inspecting the envelope correlation coefficients in Fig. 7 calculated according to (13).

Furthermore, Fig. 6 reveals that all modes are excited by one of the six antenna ports, even those which have a comparatively small modal significance. This is due to the correlation of current densities belonging to the same representation. This has the consequence that there is no further degree of freedom to realize a seventh uncorrelated antenna port.

This initial example demonstrates the consequences of symmetry on the excitation of characteristic modes. The number of orthogonal sets of characteristic surface current densities and thus the number of feasible uncorrelated antenna ports is directly related to the number and dimensions of the irreducible representations. From the representations, instructions on how to realize the excitations of the sets of modes can be deduced.

B. Square Plate with Excitation Slots

The question arises whether the symmetry analysis is also useful if a multi-mode antenna with practical excitations is considered (see e.g. [11]). To this end, a slot excitation inspired by [9] is designed for the square plate of the previous subsection. The optimized design is depicted in Fig. 8 and the corresponding feed network is shown in Fig. 9.

Although the characteristic modes will in general change by introducing excitation structures, the symmetry properties

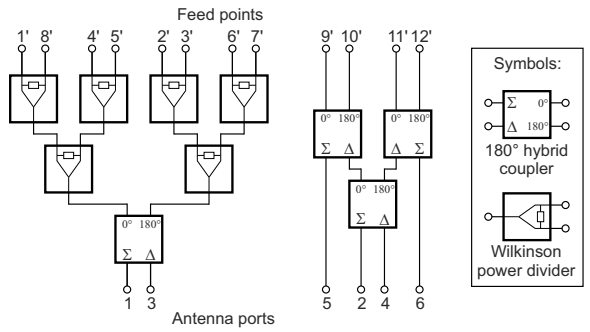

Fig. 9. Schematic of ideal feed network consisting of 180 ° hybrid couplers and Wilkinson power dividers connecting antenna ports as defined in section V-A with feed points of Fig. 8.

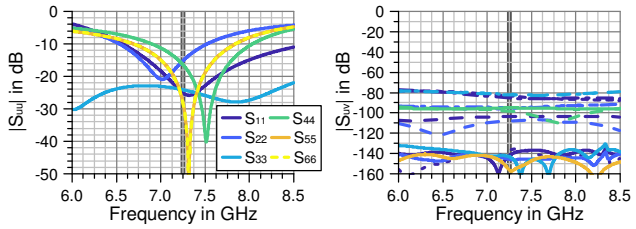

(a) (b)

Fig. 10. Simulated S-parameters of square PEC plate with excitation slots and feed network. (a) Input reflection coefficients. (b) Transmission coefficients.

of the characteristic surface current densities and hence their orthogonality are still governed by the symmetry group of the antenna. From the symmetry analysis it is thus derived that the symmetry group D_4 of the square plate has to be maintained in order to realize six uncorrelated antenna ports. Therefore, practical excitations of any sort have to be designed in such a way that the symmetry of the original structure is preserved. The excitation slots and the feed points in Fig. 8 fulfill this requirement. The positions of the slots along the edges of the plate are adopted from Fig. 5. The antenna ports 1 and 3 as defined in section V-A use the feed points $1'$ to $8'$ in Fig. 8, the antenna ports 2, 4, 5 and 6 use the feed points $9'$ to $12'$.

The antenna input ports and the feed points within the excitation slots are connected by means of the feed network shown in Fig. 9. The port configuration in Fig. 5 is used as the basis for the design of the feed network. Wilkinson power dividers and 180 ° hybrid couplers are employed in order to distribute the input signals from the antenna ports to the feed points of the plate and control the amplitude and phase relations at the feed points. The input impedances of the antenna ports are controlled by the lengths of the excitation slots and the feed positions within the slots [9].

In order to analyze the complete antenna including the feed network, a simulation in Empire XPU, which uses the FDTD-method (finite-difference time-domain), is carried out. For this purpose, the antenna is modelled according to Fig. 8 as a PEC plate in free space. The feed network is taken into account by means of a circuit simulation offered by Empire XPU using ideal Wilkinson power dividers and 180 ° hybrid couplers according to Fig. 9.

The simulated S-parameters are shown in Fig. 10. The

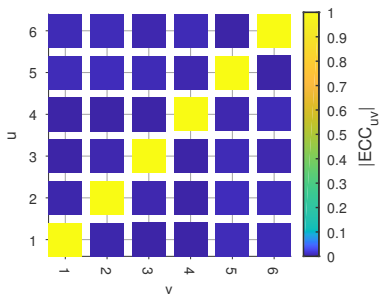

Fig. 11. Envelope correlation coefficients (ECC) of square PEC plate with excitation slots and feed network at 7.25 GHz.

lengths of the excitation slots and the feed positions within the slots are optimized so that the antenna ports are matched to 50 Ω. For antenna port 3, a quarter-wave impedance transformer with a characteristic impedance of 70.71 Ω is added at the input to achieve a better impedance match. At 7.25 GHz, all antenna ports have an input reflection coefficient of less than −15 dB (Fig. 10(a)). The transmission coefficients (Fig. 10(b)) are all well below −70 dB, demonstrating a high isolation between the antenna ports. As the feed network is ideal and the antenna is lossless, this port isolation can be attributed to the fact that the ports excite mutually orthogonal sets of characteristic modes due to the symmetry of the antenna. A slight asymmetry due to the cubic mesh in Empire XPU results in the fact that the isolation is finite.

The analysis of the S-parameters shows that the antenna ports are decoupled. Now, the envelope correlation coefficients are calculated according to (13) from the far fields simulated in Empire XPU. They are shown in Fig. 11 and confirm that the antenna ports are uncorrelated.

This example underlines that the results of the symmetry analysis still hold if a modified antenna is considered. In other words, the symmetry of the complete antenna has to be taken into account. This has the consequence that excitation elements have to be designed in such a way that the symmetry group of the complete antenna is the same as that of the original structure. From the theory it can be derived that this conclusion is valid for any type of excitation.

C. Sensitivity Analysis of Square Plate

Another question of practical importance is how sensitive the antenna ports are to small asymmetries of the antenna, which may e.g. result from the fabrication process. In order to analyze this exemplarily, one dimension of the square plate (Fig. 1) is gradually shortened. This way, the symmetry group is no longer D_4, but D_2 of order 4 (rectangular plate) [22].

The effect of this reduction of the symmetry order on the antenna with the port configuration according to Fig. 5 is evaluated by means of the envelope correlation coefficients (ECC), which are shown in Fig. 12 for different dimensions of the now rectangular plate. It is observed that the ports 1 and 3 and the ports 2 and 4 are correlated if the symmetry group is reduced. The correlation becomes more pronounced as the dimension disparity is increased. This is due to the fact that the one-dimensional irreducible representations 1

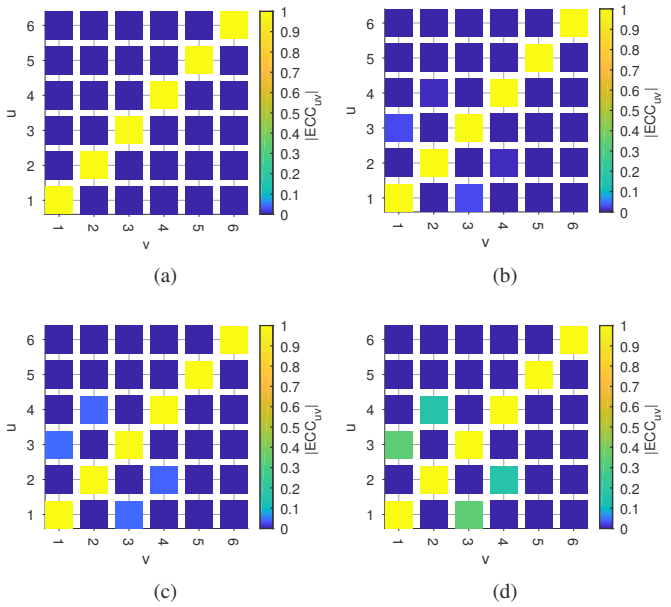

Fig. 12. Sensitivity to asymmetry of envelope correlation coefficients (ECC) of original square PEC plate excited according to Fig. 5 at 7.25 GHz. One dimension of the plate is gradually shortened in order to reduce the symmetry order (rectangle). (a) 40 mm×40 mm. (b) 40 mm×39 mm. (c) 40 mm×37 mm. (d) 40 mm×30 mm.

and 3 as well as 2 and 4 of the symmetry group of the square plate respectively collapse into one representation of the symmetry group of the rectangular plate. Therefore, the rectangular plate offers only four uncorrelated antenna ports. In general, a reduction of the symmetry order thus leads to correlated antenna ports.

However, it is also observed that for small dimension differences the port correlation is comparatively low and it increases gradually with increasing dimension disparity. With respect to the port correlation, there is apparently a smooth transition from one symmetry group to the other. These observations give rise to the conclusion that the antenna ports may be rather insensitive to small asymmetries of the antenna and the effects of small asymmetries on the port correlation may be considered negligible for practical designs.

D. Square Cuboid

The previous examples offer a maximum of six uncorrelated antenna ports. In order to increase the number of uncorrelated antenna ports, structures with higher symmetry, i.e. whose symmetry groups have more irreducible representations or irreducible representations of higher dimension, have to be used.

As an example with more complex symmetry, a perfectly electrically conducting square cuboid with dimensions 60 mm×60 mm×20 mm is now examined (Fig. 13). Its symmetry group is D_{4h} of order 16. Its first eight elements are the same as those of symmetry group D_4 of the square (proper rotations, Table I). In addition, the xy-plane acts as a mirror plane. This results in eight additional group elements which are the symmetry operations of group D_4 followed by the

TABLE IV
CHARACTER TABLE OF SYMMETRY GROUP D_{4h}

D_{4h}	E	C_{4z}	C_{4z}^{-1}	C_{2z}	C_{2x}	C_{2y}	C_{2a}	C_{2b}
$\Gamma^{(1)}$	1	1	1	1	1	1	1	1
$\Gamma^{(2)}$	1	1	1	1	−1	−1	−1	−1
$\Gamma^{(3)}$	1	−1	−1	1	1	1	−1	−1
$\Gamma^{(4)}$	1	−1	−1	1	−1	−1	1	1
$\Gamma^{(5)}$	2	0	0	−2	0	0	0	0
$\Gamma^{(6)}$	1	1	1	1	1	1	1	1
$\Gamma^{(7)}$	1	1	1	1	−1	−1	−1	−1
$\Gamma^{(8)}$	1	−1	−1	1	1	1	−1	−1
$\Gamma^{(9)}$	1	−1	−1	1	−1	−1	1	1
$\Gamma^{(10)}$	2	0	0	−2	0	0	0	0
D_{4h}	σ_{xy}	S_{4z}	S_{4z}^{-1}	I	σ_{xz}	σ_{yz}	σ_{az}	σ_{bz}
$\Gamma^{(1)}$	1	1	1	1	1	1	1	1
$\Gamma^{(2)}$	1	1	1	1	−1	−1	−1	−1
$\Gamma^{(3)}$	1	−1	−1	1	1	1	−1	−1
$\Gamma^{(4)}$	1	−1	−1	1	−1	−1	1	1
$\Gamma^{(5)}$	2	0	0	−2	0	0	0	0
$\Gamma^{(6)}$	−1	−1	−1	−1	−1	−1	−1	−1
$\Gamma^{(7)}$	−1	−1	−1	−1	1	1	1	1
$\Gamma^{(8)}$	−1	1	1	−1	−1	−1	1	1
$\Gamma^{(9)}$	−1	1	1	−1	1	1	−1	−1
$\Gamma^{(10)}$	−2	0	0	2	0	0	0	0

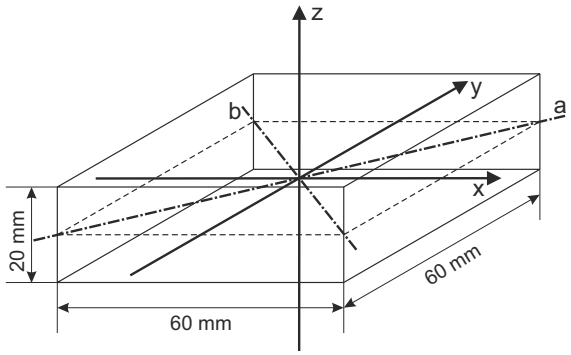

Fig. 13. Square cuboid and coordinate system.

reflection through the xy-plane σ_{xy} (improper rotations: σ denoting a reflection, S a rotoreflection and I the inversion) [22]. The 16 group elements are summarized in Table IV.

The symmetry group D_{4h} has ten irreducible representations. The corresponding characters are listed in Table IV. The fifth and the tenth representation are two-dimensional, which can be derived from the fact that the character for the identity element E is two for these representations. The two-dimensional representation matrices are not displayed here for brevity. They are taken from [20].

The first five representations can also be viewed as "even" representations as the characters (or representation matrices) of the proper rotations and the corresponding improper rotations (resulting from the proper rotations followed by the reflection through the xy-plane) are the same. In contrast, the representations 6 to 10 may be called "odd" as the characters (or representation matrices) of the improper rotations can be

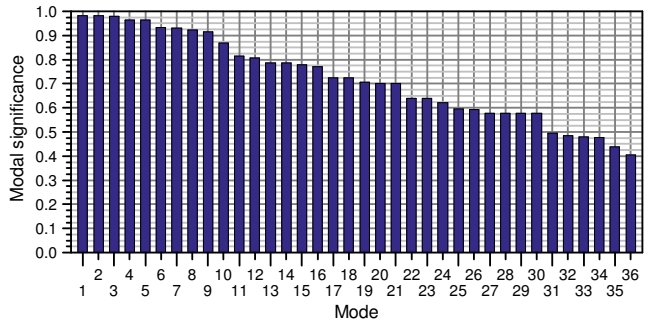

Fig. 14. Modal significances of square PEC cuboid at 7.25 GHz.

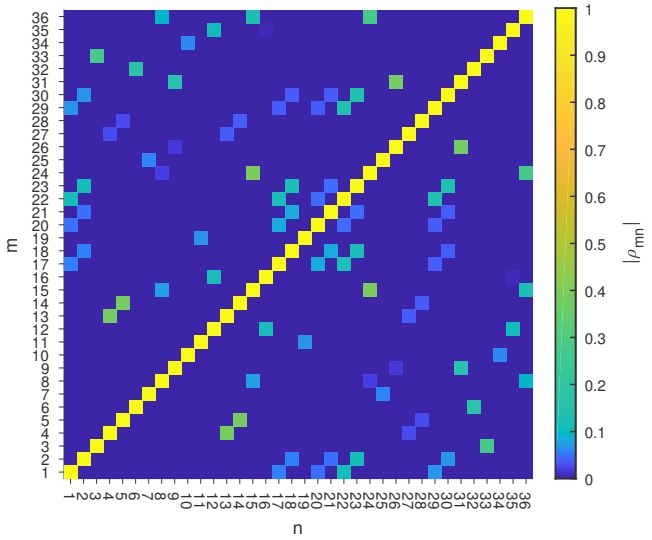

Fig. 15. Characteristic current correlation of square PEC cuboid at 7.25 GHz.

calculated from the characters (or representation matrices) of the proper rotations by multiplying them with -1.

With the symmetry analysis presented in this paper, important predictions about the characteristic modes of the square cuboid can already be made at this point. As there are eight one-dimensional and two two-dimensional representations, there are twelve sets of characteristic modes. Due to the orthogonality theorem, characteristic surface current densities belonging to different sets are orthogonal to each other. Therefore, twelve uncorrelated antenna ports may be realized by selectively exciting the modes of the different sets.

This is now verified by means of a modal analysis of the square cuboid. For this purpose, the cuboid is meshed with 4768 triangles. In Fig. 14, the modal significances of the first 36 modes are displayed. Modes 1 to 18 are considered significant. The mode pairs 1-2, 4-5, 13-14, 17-18, 20-21, 22-23, 27-28, and 29-30 are found to be degenerate. The inspection of the current correlation shown in Fig. 15 confirms that there are twelve sets of orthogonal characteristic surface current densities, as expected. Consequently, the characteristic modes can now be sorted into twelve orthogonal sets. However, they cannot be assigned to the different irreducible representations of the square cuboid based on this information alone. This can only be achieved by inspecting the surface current densities,

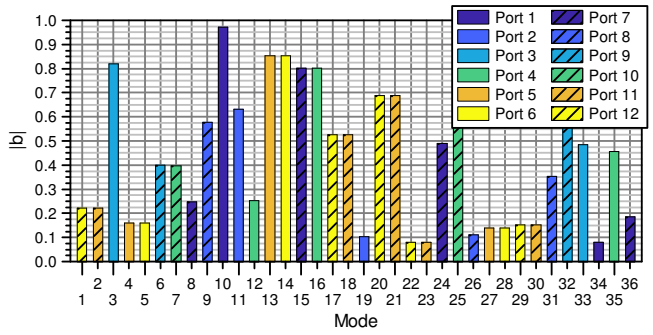

Fig. 16. Absolute values of normalized modal weighting coefficients of square PEC cuboid at 7.25 GHz.

TABLE V
ASSIGNMENT OF CHARACTERISTIC MODES OF SQUARE PEC CUBOID TO IRREDUCIBLE REPRESENTATIONS OF SYMMETRY GROUP D_{4h}

Port	Representation	Characteristic modes
1	$\Gamma^{(1)}$	10; 34
2	$\Gamma^{(2)}$	11; 19
3	$\Gamma^{(3)}$	3; 33
4	$\Gamma^{(4)}$	12; 16; 35
5-6	$\Gamma^{(5)}$	4-5; 13-14; 27-28
7	$\Gamma^{(6)}$	8; 15; 24; 36
8	$\Gamma^{(7)}$	9; 26; 31
9	$\Gamma^{(8)}$	6; 32
10	$\Gamma^{(9)}$	7; 25
11-12	$\Gamma^{(10)}$	2-1; 18-17; 21-20; 23-22; 30-29

though this step is not even necessary, as will be shown in the following paragraphs.

It is now purposeful to continue with defining the antenna ports. As already explained, the symmetry group of the square cuboid can be viewed as an evolution of the symmetry group of the square. It is therefore convenient to use the voltage sources of the square plate (Fig. 5) on the top and bottom face of the cuboid. The top face is always driven according to Fig. 5. For the first six antenna ports, the bottom face is also driven according to Fig. 5, i.e. both faces are excited in phase ("even excitation"). For ports seven to twelve, the voltage sources on the bottom plate are driven out of phase, i.e. all arrows in Fig. 5 have to be rotated by 180° ("odd excitation").

The normalized modal weighting coefficients of the square cuboid are shown in Fig. 16. Again, each antenna port excites a different set of characteristic modes. As the ports are designed as basis functions of the irreducible representations of the square cuboid, every set only consists of modes belonging to the same representation or the same row of a two-dimensional representation (cf. Fig. 15). Based on this, the characteristic modes can now be assigned to the irreducible representations without explicitly examining the surface current densities. This is summarized in Table V.

Since the antenna ports excite orthogonal sets of characteristic modes, they are uncorrelated which is confirmed by examining the envelope correlation coefficients shown in Fig. 17. As predicted, twelve uncorrelated antenna ports are

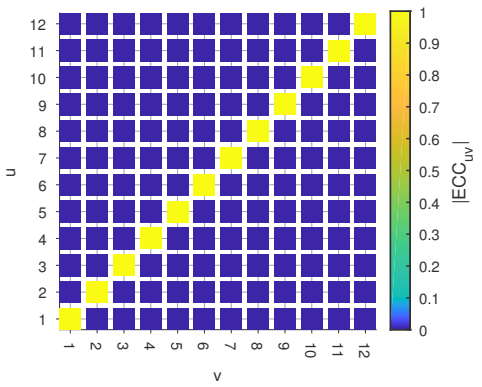

Fig. 17. Envelope correlation coefficients (ECC) of square PEC cuboid at 7.25 GHz.

realized. As all modes are already in use, there is no further degree of freedom to realize further uncorrelated antenna ports.

It should be noted that the weighting coefficients of some significant modes are comparatively low (e.g. modes 1 and 2 in Fig. 16). This is due to the actual port implementation and may have to be optimized depending on the design goals. Nevertheless, the symmetry requirements have always to be fulfilled in order to ensure decorrelation of the antenna ports.

This example highlights that the symmetry analysis yields a lot of insight into the analysis and the excitation of characteristic modes. Although the geometric structure is rather complex and there are many significant modes, predictions about the properties of the characteristic modes and how to excite them can be made without even conducting a modal analysis.

VI. Conclusion and Discussion

Symmetry analysis based on group theory and matrix representations is applied to the theory of characteristic modes in order to derive rules for the selective excitation of characteristic modes on perfectly electrically conducting antenna structures. The characteristic surface current densities act as basis functions of the irreducible representations of the symmetry group of the antenna. Those current densities belonging to different representations and those belonging to different rows of a multidimensional representation are orthogonal to each other and can thus be excited separately. Therefore, the number of feasible uncorrelated antenna ports can be predicted from the number and dimensions of the irreducible representations. In other words, there is an upper bound for the number of perfectly uncorrelated antenna ports of a given antenna geometry. In addition, the representation matrices reveal where to place feed points and how to drive them.

In Table VI, different symmetric antenna geometries are listed with their corresponding symmetry groups. The number of uncorrelated antenna ports is calculated from the number and dimensions of the irreducible representations. As an example, a cube has four one-dimensional, two two-dimensional and four three-dimensional irreducible representations [22]. The number of uncorrelated antenna ports can thus be calculated as $4 \cdot 1 + 2 \cdot 2 + 4 \cdot 3 = 20$. As a general guideline, Table VI shows that antenna structures with high symmetry, i.e. whose symmetry groups have a lot of irreducible representations or representations of higher order, are very suitable for designing multi-port antennas.

It has to be kept in mind that a sufficient number of significant characteristic modes has to be available, which is related to the electrical size of the antenna. It would thus be interesting to know whether there is an optimum antenna size if the maximum number of uncorrelated antenna ports is to be realized. For this purpose, it might be suitable to analyze geometries with circular symmetry, e.g. a circular disk (which can be considered the generalization of the square plate). Although such geometries have symmetry groups with an infinite number of elements, the basic properties introduced in this paper, in particular the orthogonality theorem for characteristic surface current densities, are still valid [20]. However, there is now an infinite number of irreducible representations [23]. This fact might be exploited to find some criteria relating the number of antenna ports to the electrical size of the antenna, which will be the topic of future research.

Another limiting factor for the realization of uncorrelated antenna ports is the feed network. The examples presented in this paper indicate that, in order for the antenna ports to act as basis functions of the representations, many feed points may have to be driven simultaneously. This may require a relatively complex feed network per port. For practical multi-port antenna designs it is therefore expected that there will be a compromise between the number of feasible antenna ports and the complexity of the feed network, depending on application and cost.

In this context, it has to be kept in mind that a practical antenna design will have some asymmetry (e.g. due to fabrication) and the feed network will have finite isolation. From the sensitivity analysis performed in this work, it is deduced that small asymmetries may only slightly affect the port correlation. (Also cf. the design in [9], which basically fulfills the symmetry requirements, but has some asymmetries introduced due to practical considerations.) In order to quantify these observations, the effects of asymmetry will be further investigated in upcoming work. Nevertheless, a great advantage of the proposed design method is that, as the antenna element itself is designed to have uncorrelated ports, correlation introduced due to imperfections in the fabrication process or in the feed and matching network are not as detrimental as in antenna designs that allow for a certain amount of port correlation from the start.

Another outcome of the numerical analyses is a relatively low correlation between certain characteristic surface current densities, though they are not perfectly orthogonal to each other according to the theory (see Fig. 4 and 15). It was also noted that the modal weighting coefficients of some significant characteristic modes may be comparatively low, depending on the actual configuration of the excitation (see Fig. 16). Based on these observations, the question arises whether even more antenna ports can be created if a certain envelope correlation is permitted. In this case, a possible approach would be to first design the (perfectly) uncorrelated antenna ports based on the symmetry of the antenna. After that, a certain threshold for the envelope correlation may be defined and more antenna ports

TABLE VI
SYMMETRY GROUP, NUMBER OF IRREDUCIBLE REPRESENTATIONS, AND NUMBER OF FEASIBLE UNCORRELATED ANTENNA PORTS FOR DIFFERENT SYMMETRIC ANTENNA GEOMETRIES

Antenna geometry	Symmetry group	No. of irreducible representations			No. of uncorrelated ports
		1-dimensional	2-dimensional	3-dimensional	
Isosceles triangular plate	C_2	2	0	0	2
Rectangular plate	D_2	4	0	0	4
Rectangular pyramid	C_{2v}	4	0	0	4
Equilateral triangular plate	D_3	2	1	0	4
Regular triangular pyramid	C_{3v}	2	1	0	4
Square plate	D_4	4	1	0	6
Square pyramid	C_{4v}	4	1	0	6
Regular hexagonal plate	D_6	4	2	0	8
Regular hexagonal pyramid	C_{6v}	4	2	0	8
Rectangular cuboid	D_{2h}	8	0	0	8
Regular triangular prism	D_{3h}	4	2	0	8
Regular tetrahedron	T_d	2	1	2	10
Square cuboid	D_{4h}	8	2	0	12
Regular hexagonal prism	D_{6h}	8	4	0	16
Cube	O_h	4	2	4	20

may be created by using those characteristic modes which are only weakly correlated with the symmetric excitations. In contrast to the port definition based on the symmetry analysis, the second step is expected to require some kind of optimization procedure.

The practical considerations raised above will be the focus of upcoming research with the aim to design prototype antennas based on the presented theory. However, they should not hide the fact that the symmetry analysis of characteristic modes is of very fundamental nature. It offers basic understanding of modal properties, especially regarding the excitation of characteristic modes. It is therefore proposed as a powerful tool to design multi-mode antennas with a higher number of antenna ports than reported so far in the literature.

REFERENCES

[1] R. Garbacz and R. Turpin, "A generalized expansion for radiated and scattered fields," *IEEE Transactions on Antennas and Propagation*, vol. 19, no. 3, pp. 348–358, May 1971.

[2] R. Harrington and J. Mautz, "Theory of characteristic modes for conducting bodies," *IEEE Transactions on Antennas and Propagation*, vol. 19, no. 5, pp. 622–628, Sep 1971.

[3] ——, "Computation of characteristic modes for conducting bodies," *IEEE Transactions on Antennas and Propagation*, vol. 19, no. 5, pp. 629–639, Sep 1971.

[4] S. K. Chaudhury, H. J. Chaloupka, and A. Ziroff, "Multiport antenna systems for MIMO and diversity," in *Proceedings of the Fourth European Conference on Antennas and Propagation*, April 2010, pp. 1–5.

[5] R. Martens, J. Holopainen, E. Safin, J. Ilvonen, and D. Manteuffel, "Optimal dual-antenna design in a small terminal multiantenna system," *IEEE Antennas and Wireless Propagation Letters*, vol. 12, pp. 1700–1703, 2013.

[6] H. Li, Z. T. Miers, and B. K. Lau, "Design of orthogonal MIMO handset antennas based on characteristic mode manipulation at frequency bands below 1 GHz," *IEEE Transactions on Antennas and Propagation*, vol. 62, no. 5, pp. 2756–2766, May 2014.

[7] R. Martens and D. Manteuffel, "Systematic design method of a mobile multiple antenna system using the theory of characteristic modes," *IET Microwaves, Antennas Propagation*, vol. 8, no. 12, pp. 887–893, Sept 2014.

[8] M. Bouezzeddine and W. L. Schroeder, "Design of a wideband, tunable four-port MIMO antenna system with high isolation based on the theory of characteristic modes," *IEEE Transactions on Antennas and Propagation*, vol. 64, no. 7, pp. 2679–2688, July 2016.

[9] D. Manteuffel and R. Martens, "Compact multimode multielement antenna for indoor UWB massive MIMO," *IEEE Transactions on Antennas and Propagation*, vol. 64, no. 7, pp. 2689–2697, July 2016.

[10] D. W. Kim and S. Nam, "Systematic design of a multiport MIMO antenna with bilateral symmetry based on characteristic mode analysis," *IEEE Transactions on Antennas and Propagation*, vol. 66, no. 3, pp. 1076–1085, March 2018.

[11] R. Martens, E. Safin, and D. Manteuffel, "Inductive and capacitive excitation of the characteristic modes of small terminals," in *2011 Loughborough Antennas Propagation Conference*, Nov 2011, pp. 1–4.

[12] N. Doose and P. A. Hoeher, "Massive MIMO ultra-wideband communications using multi-mode antennas," in *SCC 2015; 10th International ITG Conference on Systems, Communications and Coding*, Feb 2015, pp. 1–6.

[13] P. A. Hoeher and N. Doose, "A massive MIMO terminal concept based on small-size multi-mode antennas," *Transactions on Emerging Telecommunications Technologies*, vol. 28, no. 2, p. e2934, March 2015. [Online]. Available: https://onlinelibrary.wiley.com/doi/abs/10.1002/ett.2934

[14] N. Peitzmeier and D. Manteuffel, "Selective excitation of characteristic modes on an electrically large antenna for MIMO applications," in *12th European Conference on Antennas and Propagation (EuCAP 2018)*, April 2018, pp. 1–5.

[15] S. K. Chaudhury, W. L. Schroeder, and H. J. Chaloupka, "MIMO antenna system based on orthogonality of the characteristic modes of a mobile device," in *2007 2nd International ITG Conference on Antennas*, March 2007, pp. 58–62.

[16] B. Yang and J. J. Adams, "Systematic shape optimization of symmetric MIMO antennas using characteristic modes," *IEEE Transactions on Antennas and Propagation*, vol. 64, no. 7, pp. 2668–2678, July 2016.

[17] J. Knorr, "Consequences of symmetry in the computation of characteristic modes for conducting bodies," *IEEE Transactions on Antennas and Propagation*, vol. 21, no. 6, pp. 899–902, Nov 1973.

[18] K. R. Schab, J. M. Outwater, and J. T. Bernhard, "Classifying characteristic mode crossing avoidances with symmetry and energy coupling," in *2016 IEEE International Symposium on Antennas and Propagation (APSURSI)*, June 2016, pp. 13–14.

[19] K. R. Schab and J. T. Bernhard, "A group theory rule for predicting eigenvalue crossings in characteristic mode analyses," *IEEE Antennas and Wireless Propagation Letters*, vol. 16, pp. 944–947, 2017.

[20] J. F. Cornwell, *Group Theory in Physics: An Introduction*. San Diego, CA, USA: Academic Press, 1997.

[21] L. D. Landau and E. M. Lifshitz, *Quantum Mechanics: Non-Relativistic Theory*, 3rd ed., ser. Course of Theoretical Physics, vol. 3. Elmsford, NY, USA: Pergamon Press, 1977, ch. XII. The Theory of Symmetry.
[22] G. F. Koster, *Properties of the Thirty-Two Point Groups*. Cambridge, MA, USA: M.I.T. Press, 1963.
[23] M. Tinkham, *Group Theory and Quantum Mechanics*. New York, NY, USA: McGraw-Hill, 1964.
[24] J. H. Wilkinson, *The Algebraic Eigenvalue Problem*, ser. Monographs on numerical analysis. Oxford, UK: Clarendon Press, 1988.
[25] F. W. Byron and R. W. Fuller, *Mathematics of Classical and Quantum Physics*. Reading, MA, USA: Addison-Wesley, 1970, vol. 2, ch. 10 Introduction to Group Theory.
[26] D. Manteuffel, "MIMO antenna design challenges," in *2009 Loughborough Antennas Propagation Conference*, Nov 2009, pp. 50–56.
[27] E. Safin and D. Manteuffel, "Reconstruction of the characteristic modes on an antenna based on the radiated far field," *IEEE Transactions on Antennas and Propagation*, vol. 61, no. 6, pp. 2964–2971, June 2013.
[28] S. N. Makarov, *Antenna and EM Modeling with MATLAB*. New York, NY, USA: Wiley, 2002, pp. 60–62.
[29] E. Safin and D. Manteuffel, "Advanced eigenvalue tracking of characteristic modes," *IEEE Transactions on Antennas and Propagation*, vol. 64, no. 7, pp. 2628–2636, July 2016.
[30] M. Cabedo-Fabres, E. Antonino-Daviu, A. Valero-Nogueira, and M. Bataller, "The theory of characteristic modes revisited: A contribution to the design of antennas for modern applications," *Antennas and Propagation Magazine, IEEE*, vol. 49, no. 5, pp. 52–68, Oct 2007.

Nikolai Peitzmeier (S'17) was born in Lübbecke, Germany, in 1988. He received the B.Sc. and M.Sc. degrees in electrical engineering and information technology from the Leibniz University Hannover, Hannover, Germany, in 2013 and 2014, respectively.

Since then, he has been a Research Assistant with the Institute of Microwave and Wireless Systems, Leibniz University Hannover. His current research is focused on multiple-input multiple-output (MIMO) antenna systems based on the theory of characteristic modes, including beamforming and massive MIMO approaches. Further fields of interest are electromagnetic theory and simulation techniques as well as ultra-wideband (UWB) systems.

Dirk Manteuffel (M'09) was born in Issum, Germany, in 1970. He received the Dipl.-Ing. and Dr.-Ing. degrees in electrical engineering from the University of Duisburg-Essen, Essen, Germany, in 1998 and 2002, respectively.

From 1998 to 2009, he was with IMST, Kamp-Lintfort, Germany. As a Project Manager, he was responsible for industrial antenna development and advanced projects in the field of antennas and EM modeling. From 2009 to 2016, he was a Full Professor of wireless communications at Christian-Albrechts-University, Kiel, Germany. Since June 2016, he is a Full Professor and the Director of the Institute of Microwave and Wireless Systems, Leibniz-University Hannover, Hannover, Germany. His research interests include antenna integration and EM modeling for mobile communications and biomedical applications.

Dr. Manteuffel was the recipient of the Young Scientist Award of the Vodafone Foundation for Science in 2004 for his research on the analysis and design of integrated mobile phone antennas with special emphasis on the interaction with the user.